ELSEVIER

Journal of Chromatography A, 675 (1994) 129–139

JOURNAL OF CHROMATOGRAPHY A

Simultaneous use of size-exclusion chromatography and photon correlation spectroscopy for the characterization of poly(lactic acid) nanoparticles

P. Huve[a], T. Verrecchia[a], D. Bazile*,[a], C. Vauthier[b], P. Couvreur[b]

[a]*Rhone Poulenc Rorer, IBP-PHTEC, New Drug Delivery System Unit, 20 Avenue R. Aron, 92165 Antony Cedex, France*
[b]*Laboratoire de Physico-Chimie, Pharmacotechnie et Biopharmacie, URA CNRS 1218, 5 Avenue J.B. Clement, 92296 Chatenay Malabry Cedex, France*

(First received June 10th, 1993; revised manuscript received December 7th, 1993)

Abstract

Fetuin-coated poly(lactic acid) particles of size range 50–200 nm were prepared by an emulsion, microfluidization and solvent evaporation method. The separation of ^{14}C-labelled particles made with ^{125}I-labelled protein by size-exclusion chromatography (SEC) was followed by the measurement, in each collected fraction, of the average diameter of the particles by photon correlation spectroscopy, absorbance and concentrations by radioactivity counting. In one experiment, this showed that the dependence of the specific turbidity of the particles on their diameter correlated well with Mie's theory. A first approximation of the particle size distribution could also be obtained together with the separation capacities of Sepharose CL-2B and Sephacryl S1000, in addition to the amount of bound protein per unit surface area of the particles. Thus, the simultaneous use of size-exclusion chromatography and photon correlation spectroscopy was found to be a powerful tool that needed neither column dispersion function analysis nor any column standardization.

1. Introduction

Nanoparticles have attracted growing interest as site-specific drug-delivery devices. However, their use for *in vivo* administration is restricted by the fast uptake by the macrophages of the mononuclear phagocytes system [1]. Biodegradable and biocompatible poly(lactic acid)–fetuin nanoparticles have been designed to avoid this uptake. The uptake mechanism is complicated and depends greatly on the physico-chemical characteristics of the particles such as surface properties and size [2]. Hence precise characterization of the particles is required. The particle size distribution (PSD) of the nanoparticles must be known so as to be sure that there are no multiple populations of particles, each with a different behaviour. From another point of view, in order to assess the role of the coated protein layer at the surface of the nanoparticles, the amount of fetuin associated with the nanoparticles must be measured. Further, in addition to the precise characteristics of the particles, preparing such well defined nanoparticles is necessary in order to test their *in vivo* fate and to understand the uptake mechanism.

The average size of the studied particles is around 100 nm [3]. Various methods have been

* Corresponding author.

0021-9673/94/$07.00
SSDI 0021-9673(94)00159-7

proposed in order to characterize the size and the size distribution of such submicron particles populations including photon correlation spectroscopy (PCS), size-exclusion chromatography (SEC) and, more recently, field-flow fractionation (FFF). Further, the separation of the particles as a function of their size could be achieved by both SEC and Split-flow thin (SPLITT)-FFF (SFFF). However, poly(lactic acid) nanoparticles could be polydisperse in both size and density. If the size and the size polydispersity can be well described by PCS, no previous analysis of the density is necessary.

FFF appeared to be a versatile tool for submicron particle analysis. So far, two main subtechniques have been proposed, one based on multigravitational field (SFFF) and the other on a hydrodynamic separation. The use and applications of these techniques have been reviewed recently by Giddings [4]. In SFFF, the separation of the particles resulted from a balance between the size and the density or the mass of the particles. These combined effects led to a complex separation mechanism involving a steric-like elution mechanism [5], inertia [6] or lubrification forces [7] when high external fields were applied.

Thus, in order to obtain a separation of the nanoparticles as a function of their size, SEC has been prefered to SFFF. SEC is based only on a size-driven separation and does not involve density or other parameters. Further, it is inexpensive and has been in use for over a decade [8,9,10]. With SEC, the separation is not perfect, however, because of the axial dispersion of the chromatographic system, which gives a broad peak for a narrow particle size distribution (PSD) [8,10,11]. All chromatographic systems used for particle analysis may be considered as an operator (CH), defined in Eq. 1, which translates the PSD into a chromatogram. A PSD, hereafter denoted N, is a normalized function of the variable diameter ($\boldsymbol{d}_p$), that gives the proportion of particles, in number, which have this diameter. The percentage of the total number of particles whose diameters lie between $\boldsymbol{d}_p$ and $\boldsymbol{d}_p + d\boldsymbol{d}_p$ is given by $100N[\boldsymbol{d}_p]d\boldsymbol{d}_p$. Thus, a particle suspension is characterized if N and the total number of particles (or particle number concentration), n, are given.

A chromatogram is a function C of the elution volume, giving either the concentration of particles present at a volume v or the optical density (OD) induced by those particles. The operator CH which corresponds to the mathematical expression of the chromatographic system is given by the equation

$$C[v] = CH(nN)[v] \tag{1}$$

The common hypothesis for this operator (which is true for not too concentrated samples) is that particles do not interfere with each other during the process [8]. Therefore, CH is a linear operator. This means that the chromatogram obtained after the injection of a mixture of two suspensions, n_1N_1 and n_2N_2 is

$$CH(n_1N_1 + n_2N_2)[v] = n_1CH(N_1)[v] + n_2CH(N_2)[v] \tag{2}$$

Of course, this hypothesis is easy to test with three successive experiments.

In order to illustrate the effect of the axial dispersion of real systems, let us consider a perfectly monodisperse suspension, composed with 100% of particles whose diameter is exactly $\boldsymbol{d}_p$, called $\delta(\boldsymbol{d}_p)$, or Dirac distribution. The Dirac distribution has been prefered to Poisson or Gaussian models because it gives simpler equations which are sufficient for the purpose of this work. As the chromatographic system is not perfect, the chromatogram obtained will not show a sharp curve [8,10]; it is transformed by the chromatographic system into a chromatogram $CH(\delta(\boldsymbol{d}_p))[v]$, hereafter denoted $G[\boldsymbol{d}_p, v]$. The maximum of $CH(\delta(\boldsymbol{d}_p))$ is denoted $V_e[\boldsymbol{d}_p]$, V_e being the characteristic function of the system that gives the mean elution volume of a sample whose diameter is $\boldsymbol{d}_p$. As any suspension nN can be expressed as [8,11]

$$nN[\varphi] = \int_0^\infty nN[d_p]\delta(d_p)[\varphi]dd_p \tag{3}$$

then, as CH is also a continuous operator (closely related suspensions have closely related chromatograms), we have

$$CH(nN)[v] = \int_0^\infty nN[d_p]G[d_p, v]dd_p \tag{4}$$

G is called the dispersion function of the chromatographic system [8,11,12].

If the system was perfect, for a given value d_0 of d_p, $G[d_0, v]$ would be equal to $\delta(V_e[d_0])[v]$. Hence, for such a system, $CH(nN)[v] = nN[V_e^{-1}[v]]$, which means that the PSD of the suspension could be read directly from the chromatogram, whether the particle diameter at volume v is measured or is deduced from prior knowledge of V_e [10].

For systems that are not perfect, the chromatogram obtained from a detector (usually a spectrophotometer) needs further processing to retrieve the real PSD. This processing requires the knowledge of the chromatographic system axial dispersion function G, which can be calculated using suspensions with perfectly known PSD [8,9,10,12]. Of course, once the function has been calculated, any change in the chromatographic system must be avoided.

An alternative to this method is to use SEC just as a separating tool to obtain in each collection fraction a relatively monodisperse suspension, whose diameter is measured by PCS (a method that is much more accurate on monodisperse suspensions).

This paper shows that the combination of SEC and PCS allowed the dependence of the particle specific turbidity on their diameter to be obtained in a one-step experiment. Simultaneously, an approximation of the PSD of the suspension was obtained, in addition to a measure of the amount of protein bound to the nanoparticles.

2. Experimental

2.1. Materials

Methylene chloride (CH_2Cl_2) was purchased from Prolabo. Fetuin, a glycoprotein from foetal calf serum, was obtained from Sigma Chimie (F2379); it was further purified as described [13,14] (purification control by electrophoresis). ^{125}I-labelled fetuin was obtained by a classical method. Briefly, to 0.5 mCi $Na^{125}I$ (Amersham) were added, successively, 20 μl of 0.13 M phosphate buffer (pH 7.4), 5 μl of 1 mg ml^{-1} protein solution and 10 μl of 1 mg ml^{-1} chloramine T solution. Two minutes later, after shaking for 20 s, 20 μl of 0.6 mg ml^{-1} metabisulphite solution were added together with 100 μl of the same buffer. Free iodine was separated from the protein on a 3-ml G-5 column (Pharmacia–LKB).

The poly(lactic acid) used was PLA 50 from Phusis with M_r 47 000. ^{14}C-labelled PLA 50 (M_r 18 000) was purchased from DuPont (specific activity 7.8 mCi g^{-1}); it contained water-soluble fragments which where removed by water–methylene chloride partitioning (purification control by gel permeation chromatography).

2.2. Radioactivity counting

^{14}C Radioactivity counting was performed on a Beckman LS6000IC counter by mixing 0.5 ml of sample with 5 ml of Ready Solv HP (Beckman). ^{125}I radioactivity counting was performed on a Berthold LB 2111 γ-counter. When both ^{125}I and ^{14}C were counted together and if the ^{125}I activity did not exceed 5% of the ^{14}C one activity, it was checked that no interference occurred.

2.3. Preparation of nanoparticles

Nanoparticles were prepared by solvent evaporation of an oil-in-water emulsion [15]. First, 1.5 ml of methylene chloride solution containing 100 mg of the polymer (a mixture consisting of 1% labelled and 99% unlabelled PLA 50) was pre-emulsified by stirring (10 000 rpm for 1 min) in 10 ml of a 10 mg ml^{-1} fetuin aqueous solution with the aid of an Ultra-Turrax homogenizer (type T25; Bioblock). Then, the pre-emulsion was completed and homogenized with a Microfluidizer 110S (Microfluidics). In this apparatus, the pre-emulsion is pumped into a specially designed chamber in which fluid sheets interact at ultra-high velocity and pressure. Microchannels within the chamber provide an extremely focused interaction zone of turbulence causing the release of energy amid cavitation and shear forces, causing break-up of the droplets of the pre-emulsion. For the preparation of the

nanoparticles, the pre-emulsion was introduced into the microfluidizer at a pressure of 6 bar. Finally, methylene chloride present in the emulsion obtained after microfluidization was evaporated under vacuum, giving a colloidal suspension of nanoparticles which was filtered on a 1.2-μm filter.

2.4. Size-exclusion chromatography

A concentrated particle suspension (110 nm, 1 ml) was injected on to a Sepharose CL-2B-containing XK16-100 chromatographic column (100 cm × 16 mm I.D.) (Pharmacia). Elution was performed with 0.13 *M* phosphate buffer (pH 7.4) at a flow-rate of 0.1 ml min^{-1}. Fractions of 2 ml were collected automatically and analysed later. Sephacryl S1000 gel was also used under the same conditions (the Pharmacia FPLC system was used).

The sample of concentrated particle suspension was prepared according to the following procedure. Freshly prepared particles were concentrated tenfold by centrifugation: 10 ml of the suspension were centrifuged for 30 min at 25 000 rpm (4°C) in a T865 rotor, OTD Combi Sorvall ultracentrifuge. The supernatant was discarded and 1 ml of 0.13 *M* phosphate buffer (pH 7.4) was added. The particles were resuspended by gentle shearing. When accurate determination of particle concentration was needed, ^{14}C-labelled particles were used.

2.5. Particle diameter

The intensity average particle diameter of each fraction was measured by PCS. This technique measures the time-dependent light-scattering fluctuations from particles under Brownian agitation from which a correlation function is established using an autocorrelator. The characteristic translation diffusion coefficient obtained directly from this measurement is related to the size of the particles according to the Stokes–Einstein law [16]. The PCS apparatus used was a Brookaven BI 90 particle sizer. Each measurement took 3 min.

2.6. Spectrophotometry

Absorbance measurements (wavelengths from 200 to 1100 nm) were made on a Perkin-Elmer UV–Vis Lambda 2 spectrophotometer with a 1-cm optical path length quartz cell.

2.7. Computations

All calculations were made using Sigma Plot 3.01 on an IBM-compatible PC.

3. Results

The measurement of particle mean diameters in each collected fraction was performed after separation of the nanoparticle suspension (intensity average diameter 110 nm) on a Sephacryl S1000 packed column (Fig. 1). To agree with

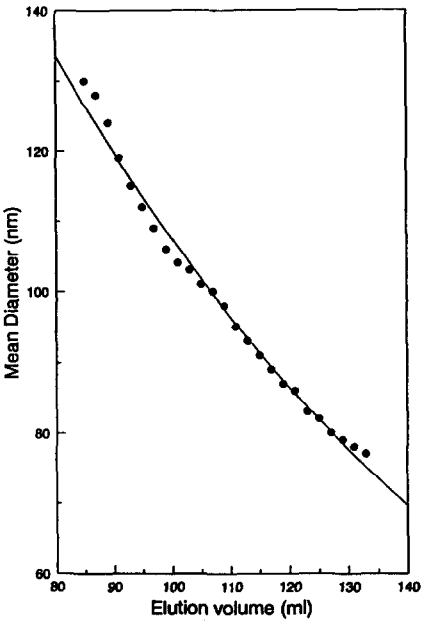

Fig. 1. Separation of 110-nm intensity average diameter PLA–fetuin nanoparticles on Sephacryl S1000 (XK16-100 column). The average diameter of the particles in each collected fraction is plotted as a function of the elution volume. The values correspond approximately ($r^2 = 0.99$) to $d = 318 \exp(-0.01086v)$, where v is the volume in ml and d the diameter in nm.

usual representation of chromatographic data, an exponential regression was calculated, giving

$$\ln d = \ln(318) - 0.01086(v) \quad (r^2 = 0.990) \qquad (5)$$

where d is the intensity average diameter (in nm) and v the elution volume (in ml).

In fact, the separation was nearly linear in the range studied, corresponding approximately to a 1-nm drop mer ml. The total volume of the column was *ca.* 200 ml but the void volume could not be determined accurately. It could be estimated to be 70 ml using 400-nm particles (results not shown).

When the same experiment was performed on Sepharose CL-2B gel with the same type of nanoparticles of 107-nm intensity average diameter, a different general shape of the curve was obtained (Fig. 2). Expecially when ln d was represented as a function of the elution volume, the superposition of two distinct slopes was obvious. The four-parameter exponential regression analysis gave

$$d = 307 \exp(-0.01087v) + 156 \exp[-0.25\ (v - 72)] \quad (r^2 = 0.997) \qquad (6)$$

This complex equation simplified into a linear expression around a 90-ml volume. Then the slope of this linear part took almost the same value as that obtained for the Sephacryl S1000 gel separation and the curves in Figs. 1 and 2 are almost superimposable. In fact, a 1-nm drop was observed for a 1-ml increase in elution volume, as for the Sephacryl S1000 gel. The total volume of the column was 200 ml, whereas the total volume of the eluent was 176 ml (determined by injection of free ^{125}I). The void volume corresponded to the transition between the two slopes at 85 ml [8].

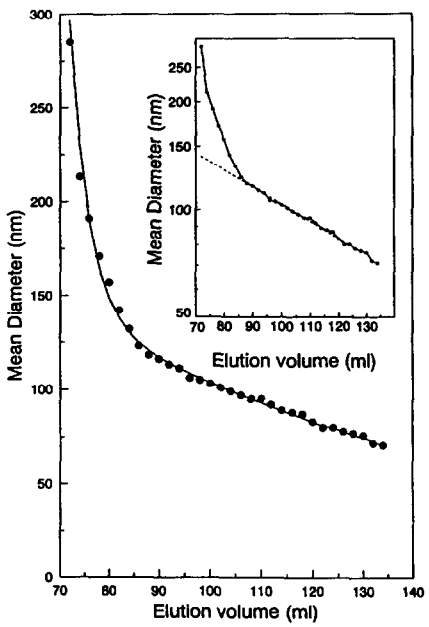

Fig. 2. Separation of 107-nm intensity average diameter PLA–fetuin nanoparticles on Sepharose CL-2B (XK16-100 column). The mean diameter of the particles in each collected fraction is plotted as a function of the elution volume. The values correspond approximately ($r^2 = 0.997$) to $d = 307 \exp(-0.01087v) + 156 \exp[-0.25\ (v - 72)]$.

In the two preceding cases, the material loss during the process was very low, and more than 99% of the expected radioactivity was recovered [8]. The Sepharose CL-2B gel was chosen because in the collected fractions, the PCS measurement indicated a much lower polydispersity value. The half-width of the 86–134 ml fraction was *ca.* 5 nm. Owing to the two separation phenomena, this gel also gave a wider diameter range. When larger particles were injected, the mean diameter measured at a given elution volume increased slightly (less than 5 nm variations), whereas a slight decrease in the mean diameter was observed after injection of smaller particles. This was in agreement with colloid SEC theory [8].

In the Sepharose CL-2B experiment (Fig. 3), the use of ^{14}C-labelled particles and the on-line measurement of the absorbance at 405 nm permitted the variation of the 405 nm absorbance/polymer concentration ratio to be represented as a function of particle diameter. This curve is compared in Fig. 4 with the calculated values obtained from ref. 17. According to Mie's theory [18], the absorbance of spherical particles in an aqueous suspension can be expressed as:

$$A = \varepsilon l C \qquad (7)$$

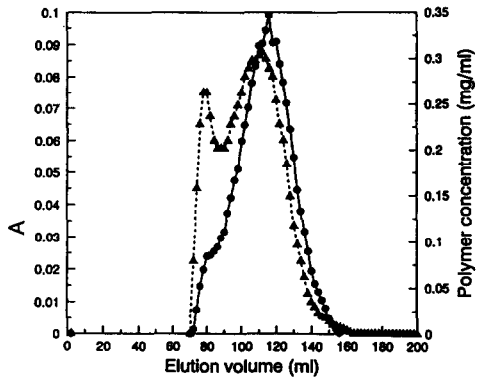

Fig. 3. Chromatograph of the separation of 107-nm ^{14}C-labelled PLA–fetuin particles by Sepharose CL-2B SEC. Absorbance at 405 nm (left-hand axis) (▲) and polymer concentration (right-hand axis) (●) are plotted *versus* the elution volume. The values of particle diameters are shown in Fig. 2.

where l is the optical path length (usually 1 cm), C is the particle mass concentration and ε is the specific turbidity, which in turn can be expressed as

$$\varepsilon = Q[d/\lambda, m(\lambda)]/\lambda \quad (8)$$

where λ is the wavelength, d the particle diameter and m their refractive index, relative to the refractive index of water. Q is a complex function and the values presented in Fig. 4 were computed assuming that the particles showed no absorbance at the wavelength studied for the indicated values of m.

The experimental values seemed to produce a curve whose shape was similar to the theoretical shape for an m value between 1.1 and 1.05. The comparison between the experimental results and theoretical values was done more precisely. In fact, in the diameter range 0–400 nm, the theoretical curves could nearly be superimposed (Fig. 5) by multiplying the ordinates by an appropriate K constant which is a function of the refractive index of the particles, m. This constant K was chosen for the refractive index of the particles $m = 1.1$ curve so as to fit the experimental data and all other K values were calculated as being the best constant to superimpose the other

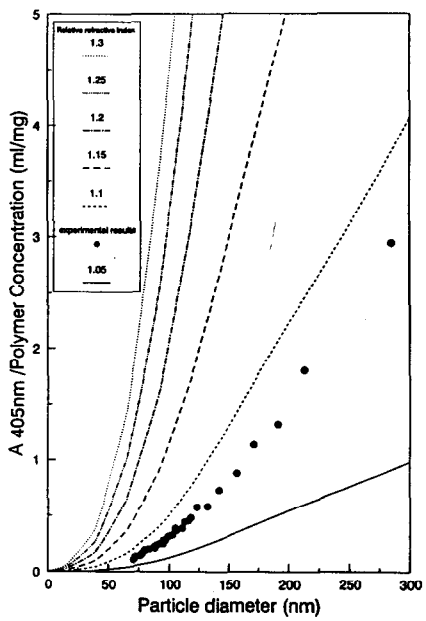

Fig. 4. Absorbance/polymer concentration ratio (proportional to specific turbidity) as a function of particle diameter. Experimental data and six theoretical curves calculated from ref. 9 with the indicated relative refractive indexes are compared.

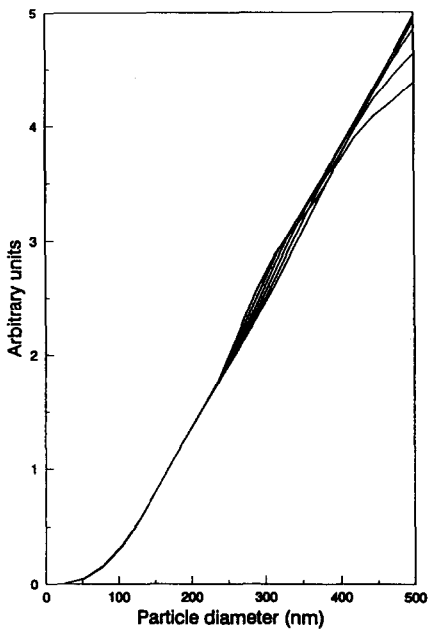

Fig. 5. Superimposition of the six previous theoretical curves after the multiplication of each of them by an appropriate $K(m)$ constant (m is the refractive index).

curves on this new curve. As the ordinates have no physical sense after the multiplication by K, "arbitrary" units were used in Fig. 5. The variation of K with m could be approximated with a third-order interpolation (Fig. 6). The superimposition of the curves, although not perfect, allowed ε to be expressed as

$$\varepsilon = K(m)F(d/\lambda)/\lambda \quad (9)$$

with only a minor approximation in the 0–400-nm diameter range. For example, in Fig. 5, in the worst case of 300-nm particles, a 1.5% error would be made by deducing the $m = 1.05$ curve from the $m = 1.1$ curve. Should the $m = 1.1$ curve be used to fit the experimental values, an even smaller error would be expected.

In order to fit the experimental data, the nearest theoretical curve ($m = 1.1$ in Fig. 4) was used. The best $K(m)$ constant was calculated and the value of m was deduced from Fig. 6 (giving $m = 1.08$). The comparison between the calculated curve and the experimental data obtained with poly(lactic acid)–fetuin nanoparticles is shown in Fig. 7. To agree with theory, the particles should be given an absolute refractive index: $1.08 \cdot 1.33 = 1.44$, where 1.33 is the refractive index of water.

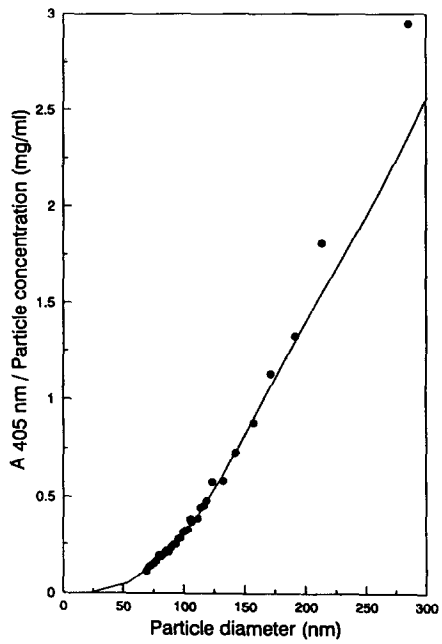

Fig. 7. Comparison between theoretical values (line) and experimental results (●). Adaptation of the $m = 1.1$ theoretical curve which gives the best fit with experimental data. The $K(m)$ constant used corresponds to a relative refractive index $m = 1.08$. The absolute refractive index of particles should be $1.08 \cdot 1.33 = 1.44$.

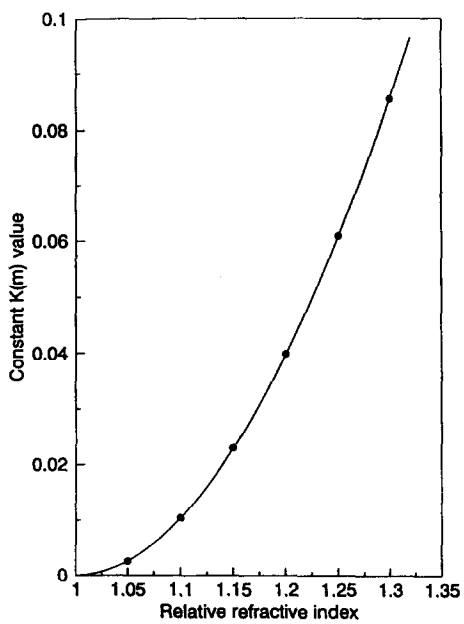

Fig. 6. Third-order interpolated curve that gives the relationship between the m and K values.

The same measurements could also be considered as a first estimation of the particle size distribution of the initial nanoparticle suspension (intensity average diameter measured by PCS of 110 nm). From Fig. 2, the diameter range could be estimated in each fraction, whereas the particle mass concentration was estimated in the same fraction using ^{14}C radioactivity measurements. As the value of the particle concentration by scattering intensity is proportional to the absorbance at 405 nm, the value of the particle concentration by number could be deduced from one of the above concentration values and from the particle diameter. For monodisperse particles the particle mass concentration M is proportional to nd^3, where d is the particle diameter and n the particle concentration by number.

To draw the PSD shown in Fig. 8, the particle concentration measured in each fraction was

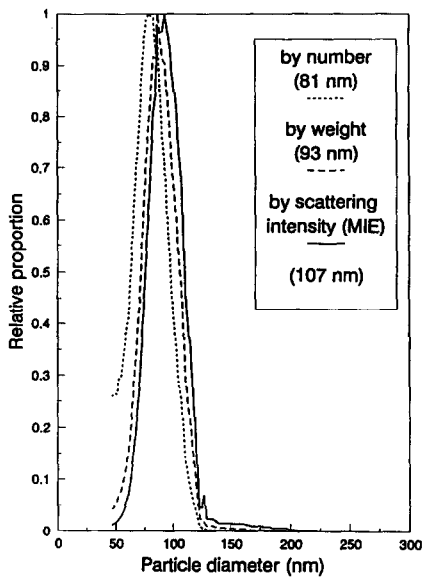

Fig. 8. First-approximation PSD deduced from experimental results. Particle concentration determined by ^{14}C counting was weighted to account for the diameter interval in the corresponding fraction (corresponding average diameter in nm). The average diameter calculated from those data were 81 nm by number, 93 nm by mass and 107 nm by scattering intensity.

divided by the width of the range of diameters in the fraction, in order to obtain the relative proportion for each size. The resulting histogram was smoothed for the sake of clarity only. The three mean diameters given in Fig. 8 were calculated using the equation

$$\text{mean diameter} = \sum dC(d) \Big/ \sum C(d) \qquad (10)$$

where C is the concentration by number, by mass or by scattering intensity and d is the diameter (in nm) [11].

Although it was not the main objective of this experiment, the use of ^{125}I-labelled fetuin allowed the measurement, in addition, of the amount of protein eluted in each fraction with the particles. As the free protein is eluted clearly after the particles (Fig. 9), it was considered that the amount of protein present in the earliest fractions corresponded to fetuin firmly bound to nanoparticles. If the amount of bound protein per unit mass of particles was represented (Fig. 10) as a function of the inverse of the particle diameter, and despite important experimental errors, a linear dependence between these parameters could be evidenced.

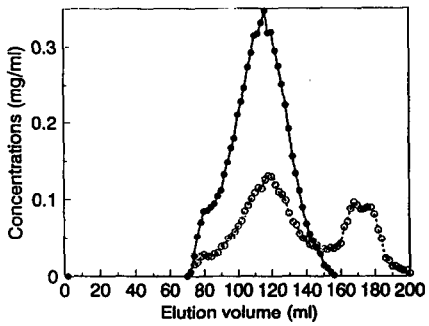

Fig. 9. Chromatograph of the separation of 107-nm ^{14}C-labelled PLA–^{125}I-labelled fetuin particles by Sepharose CL-2B SEC. ○ = Fetuin; ● = polymer concentration. The values of particle diameters are shown in Fig. 2.

4. Discussion

The main question that arises from these results is how accurate they are. In other words,

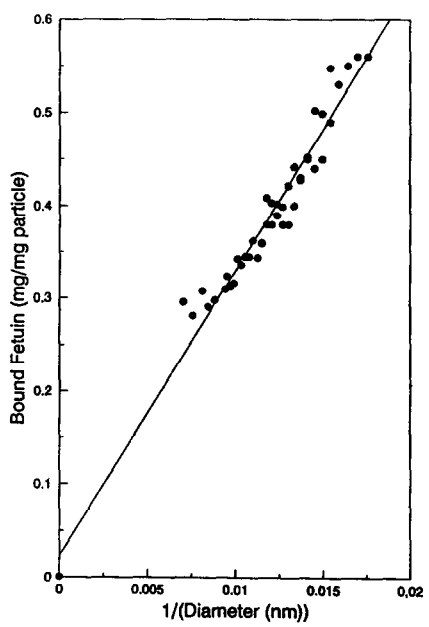

Fig. 10. Amount of bound protein per unit mass of the polymer as a function of the inverse diameter.

it is questionable if the SEC separation was sufficiently efficient to give a reliable particle PSD and an invariant curve for the variation of the particle diameter as a function of the elution volume.

The first result to be considered is the variation of the specific turbidity of the particles as a function of the diameter. A clear correlation was observed between experimental data and calculated values for $m = 1.08$ (Fig. 7). Only two experimental values corresponding to the larger particles were very erroneous owing to the very low values of both the absorbance and concentration. The relationship obtained between specific turbidity and particle diameter has been confirmed for relatively monodisperse PLA–albumin nanoparticles (not shown). No difference was noted compared with monodisperse PLA–fetuin nanoparticles. This means that the nature of the protein did not really matter as the absorbance of this protein was negligible at 405 nm. This relationship can now be used as a method to evaluate the nanoparticle concentration, with a 0.03 mg ml^{-1} accuracy for 100-nm particles. It could also be used as a measure of particle diameter if the concentration is known.

However, one drawback of this method is the need to have no specific absorbance at the wavelength used. However, even though the method has been standardized for a 405-nm wavelength, the curve can be used at any other wavelength. In fact, $\varepsilon = K(m)F(d/\lambda)/\lambda$ (Eq. 9) and the standardized curve is

$$\varepsilon = f_{405}(d) = K(m)F(d/405)/405 \quad (11)$$

If λ has to be changed:

$$\varepsilon = f_{405}(405d/\lambda) \cdot 405/\lambda \quad (12)$$

This means that the value of ε at λ may be obtained for particles whose diameter is d by calculating the value of ε at 405 nm for particles whose diameter is $405d/\lambda$ and then multiplying this value by $405/\lambda$. As the absorbance (200–1100 nm) of each fraction has been measured and when this value was large enough, Eq. 12 was easily confirmed for λ (350–1100 nm). For $\lambda < 350$ nm the absorbance of the protein was found to be no longer negligible (results not shown). In the same way, Eq. 12 could be used for particles larger than 500 nm for which the approximation made that $Q[d/\lambda, m(\lambda)]/\lambda = K(m)F(d/\lambda)/\lambda$ was no longer valid at $\lambda = 405$ nm. Hence it is only necessary that $405d/\lambda < 500$ nm. Then, the only limitation remains to maintain a sufficient signal at high wavelength.

Another drawback of the proposed method for particle concentration determination is much more difficult to bypass as it concerns its sensitivity to the polydispersity of the measured sample. For example, in the case of a 1 g l^{-1} mixture of 100- and 150-nm diameter particles in equal proportions, the absorbance at 405 nm is $A = 0.5[0.32 + (0.32 \cdot 1.5^2)] = 0.52$ and the intensity average diameter becomes $[100 + (150 \cdot 1.5^2)]/(1 + 1.5^2) = 135$ nm; ε read on the curve is then 0.56 l g^{-1} cm^{-1}. This gives a measured concentration value of 0.9 g l^{-1} instead of 1 g l^{-1}, *i.e.*, a 10% error. In fact, owing to its great sensitivity to polydispersity, this law should not be used for polydisperse samples. However, as the results obtained correlated well with the theory, it was concluded that the particle population in each fraction was not too polydisperse. This was further confirmed by photon correlation measurements that gave in each fraction a very low value for polydispersity. This showed that G was probably a skewed function.

In a second step, it should be highlighted that the curves plotted in Figs. 1 and 2 represent only an approximation of the universal calibration curve $\boldsymbol{d}_p = V_e^{-1}(v)$ of the two gels used. The values of diameters that are plotted as a function of v are the PCS intensity average diameters measured in the collected fractions. As such, and according SEC theory [9], they should depend on the nature of the injected suspension. Indeed, experimentally, changing the nature of the injected suspension did change the obtained $\boldsymbol{d}_p$–v relationship, but at most 5-nm variations were observed. A universal curve would be obtained only by injecting perfectly monodisperse samples, each of a well defined diameter. This goal could be achieved, for example, by re-injecting each collected fraction and re-measuring its PSD. However, this was not possible experimentally because, under these conditions, too low ab-

sorbance values would have been obtained. Indeed, if the collected fraction at a given volume v was injected again indefinitely, the value of the diameter in the volume v fraction would converge exactly to $V_e^{-1}(v)$. This means that what has been done here is the first step of a converging process. This means that the average diameter measured in each fraction was probably approximately equal to the standard value. Hence the injection of a single suspension with a broad distribution was sufficient to obtain a good approximation of the column standard calibration graph. Therefore, it is an easy method for standardizing SEC.

A further analysis of Figs. 1 and 2 highlighted that in the case of Sepharose CL-2B, the double-sloped curve was typical of two phenomena: for particles smaller than 125 nm, efficient separation by SEC occurred, whereas two effects are responsible for the separation of the large particles: the usual SEC separation and hydrodynamic separation [8,9,10]. We cannot exclude SEC separation of the large particles because a small proportion of large pores exists in the gel in any case. Further, the numerical results obtained showed that Sephacryl S1000 has only slightly larger pores than Sepharose CL-2B, which is in agreement with their respective standard dextran separation capacities (Pharmacia data).

The next question, which is not totally independent of the above considerations, deals with the reliability of the PSD determination. Of course, to have access to the real PSD, each fraction should have been re-injected and its own PSD determined again, in a converging process. As the measured diameter in a given fraction v was close to $V_e^{-1}(v)$, it could be concluded that the PSD obtained was certainly close to the real value. As a confirmation of this, it should be mentioned that the intensity average diameter calculated from SEC and PCS data (107 nm) was equal to the diameter measured before injection by PCS (107 nm). As generally supposed [8,10], the experimental PSD was found to be close to a log-normal distribution.

Finally, SEC was used to determine the amount of protein bound to nanoparticles. However, as the amount of ^{125}I used was low (in order not to interfere with other measurements), there was a great experimental dispersion, partially balanced by the large number of experimental data. The amount of protein bound per unit mass of polymer was found to be inversely proportional to the particle diameter. This result confirmed previous experiments performed with human serum albumin–PLA particles [3]. This proportionality means that the total amount of bound protein was also proportional to the specific surface area of the particles. With fetuin, the slope of the curve gave approximately 7 mg of bound protein per square metre of particle surface, which was twice the value found with albumin after desorption. This observation could be explained by the affinity of fetuin for itself. It was noteworthy that after desorption and washing, approximately half of the initially bound fetuin remained associated with the polymer. The final values, after washing, of the amount of bound protein are then the same for fetuin and albumin [3]. The fact that this constant proportion of protein remained bound on particles is probably the reason why no particle aggregation upset the experimentation.

5. Conclusions

The present results have shown that the combination of SEC, PCS and turbidity measurements may be considered as an alternative to the mathematical standardization of SEC for the characterization of colloidal suspensions. This method was found to be easy to use, fast and needed no rigorous column maintenance. However, concentrated samples were needed in order to obtain a sufficient signal for PCS measurements. This method has been applied to study the light scattering of colloidal particles, which was found to correlate well with Mie's theory. The resulting calibration graph could be used to determine the concentration of monodisperse particle samples with a known diameter. Also, an accurate approximation of PSD was obtained. Finally, the separation of the particles by SEC, followed by PCS and radioactivity counting in

each fraction, is proposed for determining the amount of ^{125}I-labelled protein bound to the nanoparticles.

6. References

[1] L. Illum and S.S. Davis, in P. Buri and A. Gumma (Editors), *Drug Targeting*, Elsevier, Amsterdam, 1985, pp. 65–80.
[2] R.L. Juliano, *Adv. Drug Delivery Rev.*, 2 (1988) 31–54.
[3] T. Verrecchia, P. Huve, D.V. Bazile, M. Veillard, G. Spenlehauer and P. Couvreur, *J. Biomed. Mater. Res.*, 27 (1993) 1019–1028.
[4] J.C. Giddings, *Science*, 260 (1993) 1456–1465.
[5] S. Lee and J.C. Giddings, *Anal. Chem.*, 60 (1988) 2328.
[6] J. Pazourek and J. Chmelik, *Chromatographia*, 35 (1993) 591–596.
[7] P.S. Williams, T. Koch and J.C. Giddings, *Chem. Eng. Commun.*, 111 (1992) 121.
[8] A. Penlidis, A.E. Hamielec and J.F. MacGregor, *J. Liq. Chromatogr.*, 6 (1983) 179–217.
[9] M.G. Styring, J.A.J. Honig and A.E. Hamielec, *J. Liq. Chromatogr.*, 9 (1986) 3505–3541.
[10] T. Kourti, A. Penlidis, A.E. Hamielec and J.F. MacGregor, *Polym. Mater. Sci. Eng.*, 53 (1985) 147–151.
[11] A.E. Hamielec, *J. Chromatogr. Sci.*, 25 (1985) 117–160.
[12] T. Ishige, S.-I. Lee and A.E. Hamielec, *J. Appl. Polym. Sci.*, 15 (1971) 1607–1622.
[13] J. Marti and S. Aliau, *Biochim. Biophys. Acta*, 303 (1973) 348–359.
[14] D.S. Salomon, M. Bano, K.B. Smith and W.R. Kidwell, *J. Biol. Chem.*, 257 (1982) 14093–14101.
[15] D.V. Bazile, C. Ropert, P. Huve, T. Verrecchia, M. Marlard, A. Frydman, M. Veillard and G. Spenlehauer, *Biomaterials*, 13 (1992) 1093–1102.
[16] A. Einstein, *Investigation on the Theory of the Brownian Movement*, Dover, New York, 1956.
[17] W. Heller and W.J. Pangonis, *J. Chem. Phys.*, 26 (1957) 498–506.
[18] G. Mie, *Ann. Phys. (Leipzig)*, 25 (1908) 377–445.